JOURNAL OF NATURAL PRODUCTS

Article

pubs.acs.org/jnp

Activation and Inhibition of Thermosensitive TRP Channels by Voacangine, an Alkaloid Present in *Voacanga africana*, an African Tree

Yuko Terada,[†] Syunji Horie,[‡] Hiromitsu Takayama,[§] Kunitoshi Uchida,[⊥] Makoto Tominaga,[⊥] and Tatsuo Watanabe*[,†]

[†]Graduate School of Nutritional and Environmental Sciences, University of Shizuoka, 52-1 Yada, Suruga-ku, Shizuoka 422-8526, Japan

[‡]Laboratory of Pharmacology, Faculty of Pharmaceutical Sciences, Josai International University, 1 Gumyo Togane, Chiba 283-8555, Japan

[§]Department of Biofunctional Molecular Chemistry, Graduate School of Pharmaceutical Sciences, Chiba University, 1-33 Yayoi-cho, Inage-ku, Chiba 263-8522, Japan

[⊥]Division of Cell Signaling, Okazaki Institute for Integrative Bioscience, National Institutes of Natural Sciences, Higashiyama 5-1, Myodaiji, Okazaki, Aichi 444-8787, Japan

ABSTRACT: Voacangine (**1**) is an alkaloid found in the root bark of *Voacanga africana*. Our previous work has suggested that **1** is a novel transient receptor potential vanilloid type 1 (TRPV1) antagonist. In this study, the agonist and antagonist activities of **1** were examined against thermosensitive TRP channels. Channel activity was evaluated mainly using TRP channel-expressing HEK cells and calcium imaging. Herein, it was shown that **1** acts as an antagonist for TRPV1 and TRPM8 but as an agonist for TRPA1 (EC_{50}, 8 μM). The compound competitively blocked capsaicin binding to TRPV1 (IC_{50}, 50 μM). Voacangine (**1**) competitively inhibited the binding of menthol to TRPM8 (IC_{50}, 9 μM), but it showed noncompetitive inhibition against icilin (IC_{50}, 7 μM). Moreover, the compound selectively abrogated chemical agonist-induced TRPM8 activation and did not affect cold-induced activation. Among these effects, the TRPM8 inhibition profile is unique and noteworthy, because to date no studies have reported a menthol competitive inhibitor of TRPM8 derived from a natural source. Furthermore, this is the first report of a stimulus-selective TRPM8 antagonist. Accordingly, **1** may contribute to the development of a novel class of stimulus-selective TRPM8 blockers.

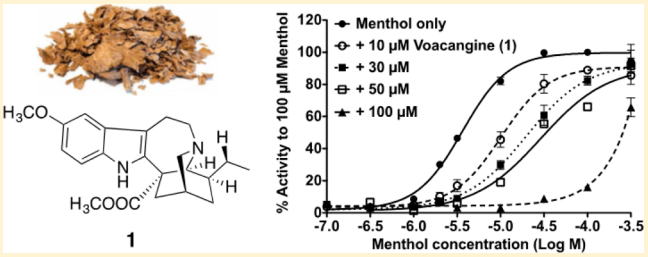

Voacangine (**1**) is an alkaloid found in the root bark of *Voacanga africana* Stapf ex Scott-Elliot (Apocynaceae) and is characterized by the presence of an iboga middle ring-containing moiety. *V. africana* is a widely distributed tree in West Africa, Congo, and Tanzania. In Côte d'Ivoire, an infusion of the root bark is used for the treatment of diarrhea, leprosy, generalized edema, convulsions in children, and madness.[1] In addition, practitioners of traditional medicine in Cameroon have suggested that *V. africana* possesses antiulcer properties.[2] Furthermore, aqueous and methanol extracts of the root bark exert protective effects against hydrochloric acid (HCl)/ethanol-evoked gastric ulcers in rats.[3,4] From these data, it is speculated that the root bark of *V. africana* may contain antidiarrheal components. However, the effective components of *V. africana* have not been identified, and human experiments have not been reported.

The transient receptor potential vanilloid type 1 (TRPV1), also known as the capsaicin (CAP) receptor, belongs to the TRP family of nonselective cation channels.[5] TRPV1 responds to multiple noxious stimuli, including CAP (the pungent component of chili peppers),[5] heat (temperatures ≥43 °C),[5] and low pH (pH ≤5.9).[6] TRPV1 is expressed in sensory neurons throughout the body, including the dorsal root ganglion (DRG) and nodose ganglion neurons in nerve fibers and in the gastrointestinal tract.[6−8] In the gut, TRPV1 participates in the regulation of gastrointestinal motility, blood flow, secretion, mucosal homeostasis, and nociception.[9−11] CAP has been used to investigate gastrointestinal motility involving TRPV1.[12]

Recently, our group investigated the effect of the methanol extract of the root bark of *V. africana* on CAP-induced smooth muscle contraction using mouse rectum, where TRPV1-immunoreactive fibers are abundant. The extract inhibited CAP-evoked contraction of the rectum, and the main active component was identified as voacangine (**1**). Activation of muscarinic M_3 receptors and nicotinic receptors also could be involved in the CAP-induced contraction of smooth muscle,

Received: October 20, 2013
Published: January 31, 2014

but **1** did not block these. These results raised the possibility that **1** prevents contraction of the rectum by blocking TRPV1.[13] Therefore, it was hypothesized that the antidiarrheal activity of *V. africana* is elicited by a **1**-induced TRPV1 blockade. To investigate this hypothesis, the TRPV1 inhibitory potency of **1** was measured using TRPV1-expressing cells and DRG neurons. In addition, the agonistic and antagonistic activities of this compound were evaluated against other thermosensitive TRPs (TRPM8, TRPA1, TRPV2, and TRPV3).

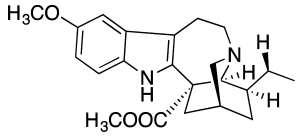

1

RESULTS AND DISCUSSION

Voacangine (1) Is an Antagonist for TRPV1 and TRPM8 but an Agonist for TRPA1. The agonistic and antagonistic effects of administration of 100 μM **1** to each TRP channel (TRPV1, TRPM8, TRPA1, TRPV2, and TRPV3)-expressing HEK cells were examined. In terms of agonistic activity, compound **1** triggered Ca^{2+} influx on TRPA1-expressing cells but not on the other TRPs. This response was significantly attenuated by preincubation with a TRPA1 antagonist, HC-030031 (Figure 1C). When antagonistic activity was considered, compound **1** not only suppressed CAP-induced TRPV1 activation but also suppressed menthol- and icilin-induced TRPM8 activation (Figure 1A and B). Compound **1** did not show an inhibitory effect on other TRPs.

These results indicated that **1** is an antagonist to TRPV1 and TRPM8 and agonist to TRPA1. Its antagonistic and agonistic activities were analyzed in detail in the following experiments.

Voacangine (1) Competitively Inhibits the Binding of CAP on TRPV1. The Ca^{2+} responses induced by 0.003 and 0.01 μM CAP after addition of 10−100 μM **1** and 10−50 μM TRPV1 antagonist 4-(3-chloro-2-pyridinyl)-*N*-[4-(1,1-dimethylethyl)phenyl]-1-piperazinecarboxamide (BCTC) or capsazepine (CPZ) to hTRPV1-expressing HEK cells are shown in Figure 2A. The representative $[Ca^{2+}]_i$ changes elicited by CAP (0.01 μM for HEK and 0.1 μM for DRG) and compound **1** (30, 100 μM for HEK and 100 μM for DRG) on HEK cells (Figure 2B) and primary cultured rat DRG neurons (Figure 2C) are shown. Compound **1** attenuated CAP-induced TRPV1 activation in both types of cells. Furthermore, its inhibitory effect was completely reversed by a washout treatment (Figure 2A). The concentration−response curves using 0.0001−10 μM CAP after addition of 10−100 μM **1** to the HEK cells are shown in Figure 2D. Compound **1** showed a dose-dependent suppression of response by CAP. In the presence of each concentration of compound **1**, the dose−response curves for CAP were shifted to the right, but their maximum responses were slightly changed (Figure 2D). These results indicate that **1** competitively inhibited CAP on TRPV1. To elucidate the mode of inhibition, a Schild plot analysis was conducted (10, 30, 50 μM **1** was used). Six series of Schild plots from six series of CAP dose−response curves were obtained, and the mean results are shown in Figure 2E. A linear regression was observed, and the slope was 1.1 ± 0.3; the slope was not significantly different from 1.0 (paired *t*-test). These results clearly showed that **1** is a competitive antagonist and that **1** and CAP act at the same recognition site on hTRPV1. The affinity of compound **1** to the CAP-binding site is shown as pA_2 = 4.7 ± 0.1 and K_B = 18 μM (Figure 2E).

Subsequently, the IC_{50} value of compound **1** was compared with those of the representative TRPV1 antagonists CPZ and BCTC. The dose-dependent inhibition curves obtained using antagonists against 0.01 μM CAP are shown in Figure 3, and their IC_{50} values are shown in Table 2. Owing to its low water solubility, **1** could not be tested at concentrations higher than 100 μM. The IC_{50} value of compound **1** was 300 times and 300 000 times larger than those of CPZ and BCTC, respectively. Compound **1** was shown to be a TRPV1 antagonist, but when compared to the synthetic antagonists, it showed a weak potency against CAP-induced TRPV1 activation.

Voacangine (1) Selectively Blocks CAP- and Heat-Induced Activation of TRPV1. The Ca^{2+} influx induced by heat of the TRPV1-expressing HEK cells after preincubation with compound **1**, BCTC, and CPZ is shown in Figure 4A. No Ca^{2+} responses were observed in HEK293T (not expressing TRPV1) cells when they were stimulated by heat (data not shown). All of the antagonists blocked heat-induced TRPV1 activation on the HEK cells, and **1** dose-dependently abrogated the responses by heat with an IC_{50} value of 24 μM (Figure 4B).

Inhibitory effects of **1**, BCTC, and CPZ for proton-induced activation of the TRPV1-expressing HEK cells are shown in Figure 4C. No responses were observed in the HEK293T cells (data not shown). BCTC and CPZ (10 μM) completely blocked proton-induced activation, but **1** barely suppressed the response at all test concentrations used (Figure 4C). The typical fluorescence changes obtained are shown in Figure 4D. BCTC completely inhibited proton-induced Ca^{2+} influx at 10 μM. In contrast, 100 μM **1** had no inhibitory effect against proton-mediated response. These results showed that **1** selectively blocks CAP- and heat-induced activation but does not inhibit proton-evoked activation of hTRPV1.

In the present study, a Schild plot analysis showed that **1** and CAP compete with each other for a high-affinity site at the TRPV1. It is reported that CAP binds to an intracellular portion of the transmembrane region 3 (TM3) of TRPV1,[14−16] so the binding site of **1** is speculated to be in TM3. However, more experiments are necessary to identify its binding sites on TRPV1.

Voacangine (1) Is the First Naturally Occurring TRPM8 Antagonist That Competes with Menthol. The Ca^{2+} response induced by 10 μM menthol and 0.3 μM icilin after preincubation with 3−50 μM **1** on mTRPM8-expressing HEK cells is shown in Figures 5A and 6A. The representative $[Ca^{2+}]_i$ changes elicited by 10 μM menthol and 0.3 μM icilin after pretreatment of HEK cells with 30−50 μM **1** are shown in Figures 5B and 6B. Compound **1** attenuated menthol- and icilin-induced TRPM8 activation in the HEK cells. Furthermore, its inhibitory effect was completely reversed by a washout treatment (Figures 5A and 6A).

Next, concentration−response curves were obtained and Schild plot analyses were conducted. The dose−response curves obtained by using 0.1−300 μM menthol and 0.01−10 μM icilin after addition of 5−100 μM **1** to the TRPM8-expressing HEK cells are shown in Figures 5C and 6C. Compound **1** dose-dependently abrogated Ca^{2+} uptake by menthol and icilin. The menthol concentration−response curves were shifted to the right, and the top responses were slightly decreased in the presence of high concentrations of **1**

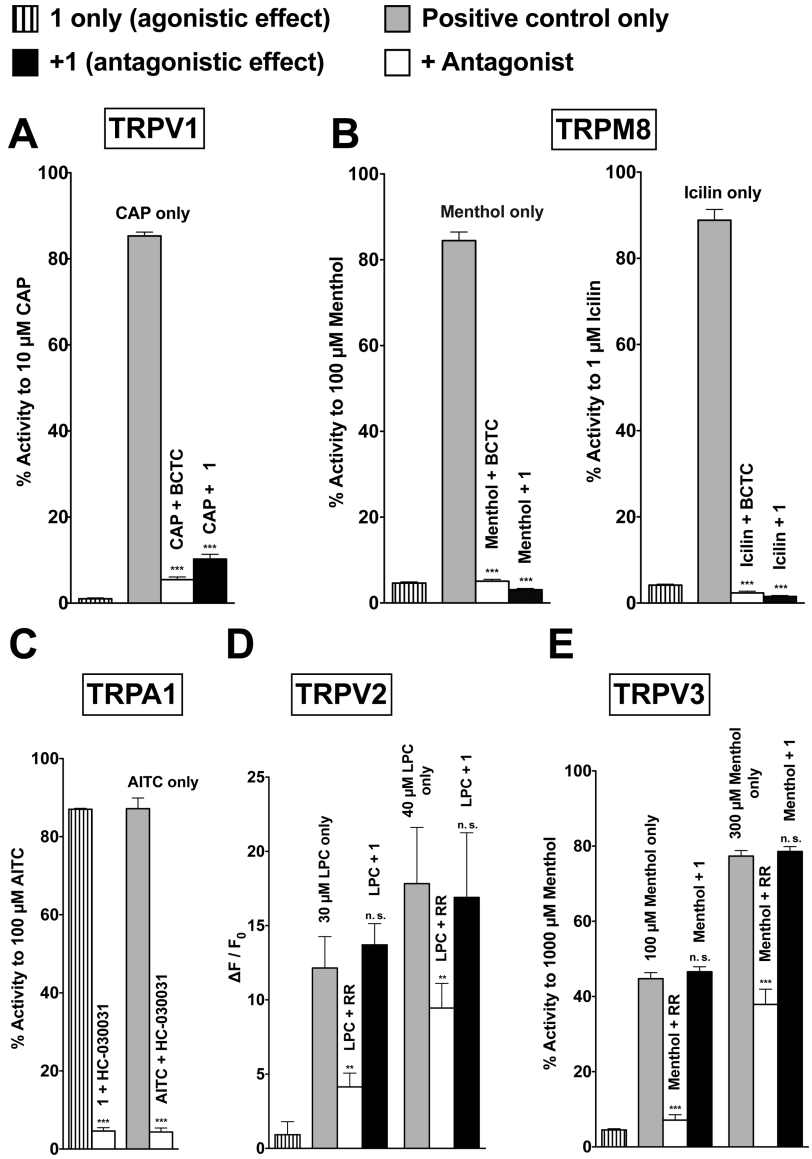

Figure 1. Agonistic and antagonistic activities of voacangine (**1**) against each TRP channel. Ca^{2+} responses on TRPV1 (A), TRPM8 (B), TRPA1 (C), TRPV2 (D), and TRPV3 (E) are shown. Except for TRPV2, data were expressed as percentages of the response to each positive control: 10 μM CAP (A), 100 μM menthol and 1 μM icilin (B), 100 μM AITC (C), 1000 μM menthol (E). The responses of TRPV2 are shown as $\Delta F/F_0$ (%). Vertically striped columns, response by 100 μM **1** only; gray-colored columns, activation by each agonists: 0.01 μM CAP (A), 10 μM menthol and 0.3 μM icilin (B), 1 μM AITC (C), 30 and 40 μM LPC (D), 100 and 300 μM menthol (E); unfilled columns, antagonism by each antagonist against the above concentration of the agonists: 10 μM BCTC (A, B), 30 μM HC-030031 (C), 5 μM RR (D, E); filled column, inhibitory effect of 100 μM **1** for the above agonists. In the antagonist assay, each antagonist and **1** were pretreated with the cells before the addition of each agonist. Each data point represents the mean ± SEM, n = 4–12. *** and n. s. indicate $p < 0.0005$ and not significant, respectively (unpaired t-test).

(Figure 5C). It was then examined as to whether higher concentrations of menthol (>300 μM) would cancel the repression of the menthol top response induced by 100 μM **1**. However, when menthol was administered at concentrations higher than 300 μM, the compound caused a nonspecific response that hindered the evaluation of the effects of **1**. In contrast, the maximum responses by icilin were drastically reduced by the addition of **1** (Figure 6C). These results indicated that compound **1** competitively inhibits the binding of menthol but noncompetitively inhibits the binding of icilin. Five series of Schild plots were conducted for the agonists, and the mean plots are displayed in Figures 5D (menthol) and 6D (icilin). For a Schild plot analysis, 10, 30, and 50 μM **1** for menthol and 10, 20, and 30 μM **1** for icilin were used. The analyses yielded slopes of 1.1 ± 0.0 for menthol and 2.4 ± 0.2 for icilin. The regression lines for both agonists were straight, and the slope for menthol did not differ significantly from 1.0 (paired t-test), but the slope for icilin differed significantly (paired t-test). Therefore, it was found that **1** is a competitive antagonist for menthol and is a noncompetitive antagonist for icilin. Menthol and icilin have different binding sites on TRPM8,[17−19] and the present results are consistent with findings reported in previous studies. The affinity of **1** to the menthol-binding site is shown as $pA_2 = 5.1 \pm 0.1$ and $K_B = 8.5$ μM (Figure 5D).

Next, the IC_{50} values of **1** were compared with those of known TRPM8 antagonists for menthol and icilin. BCTC and CPZ were used as representative synthetic antagonists and

dx.doi.org/10.1021/np400885u | J. Nat. Prod. 2014, 77, 285−297

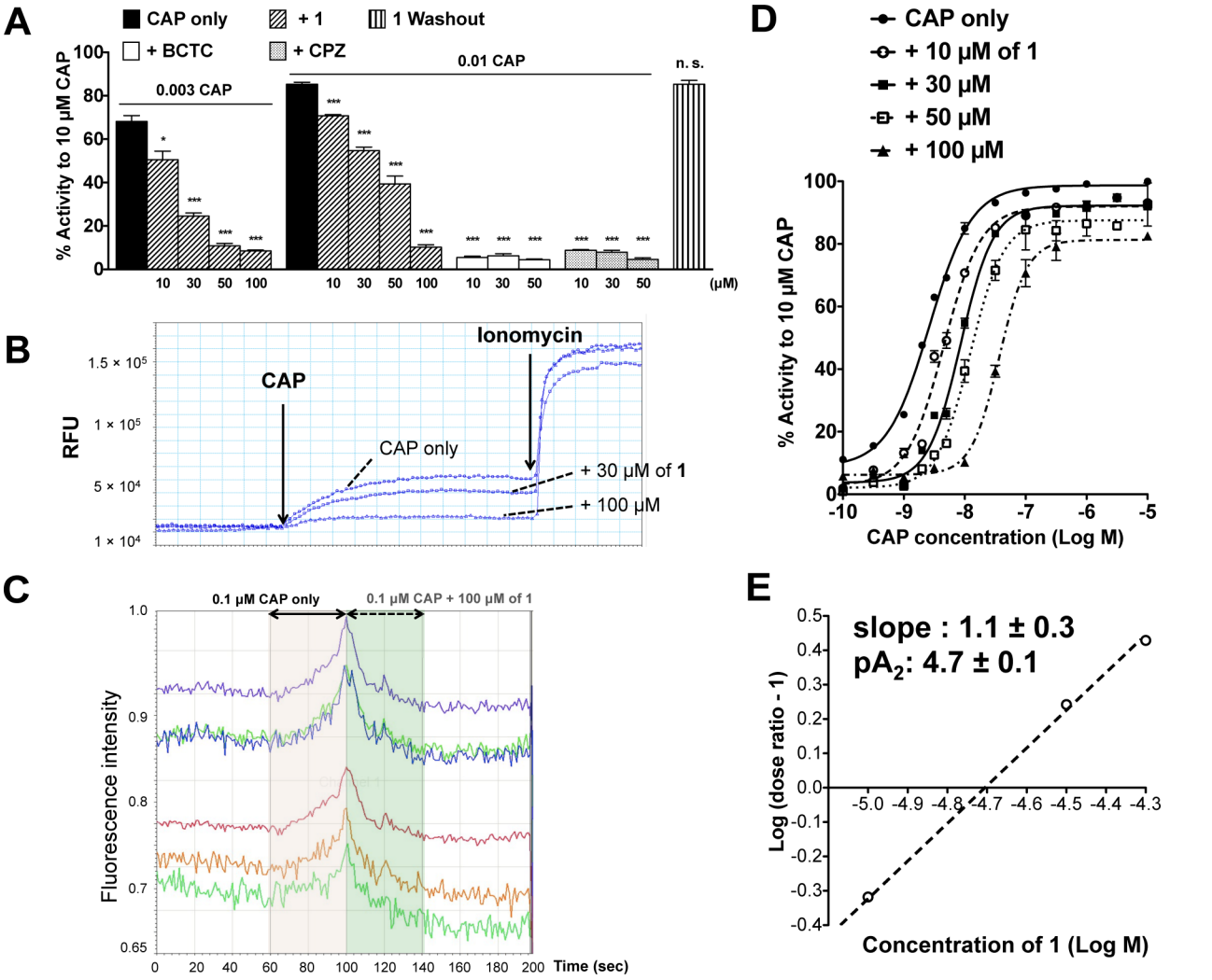

Figure 2. Suppressive effect of voacangine (**1**) against CAP-induced TRPV1 activation. Ca^{2+} influx on TRPV1-expressing HEK cells (A, B, D) and DRG neurons (C) and Schild plot for TRPV1 (E) are shown. Data values are expressed as a percent response to 10 μM CAP. (A) Filled column, TRPV1 activation by 0.003 and 0.01 μM CAP; other bars show TRPV1 activation induced by 0.003 and 0.01 μM CAP with preadministration of the following antagonists: hatched column, 10, 30, 50, and 100 μM **1**; unfilled column, 10, 30, and 50 μM BCTC; dotted column, 10, 30, and 50 μM CAP. Vertical striped column, TRPV1 activation by 0.01 μM CAP. Before addition of CAP, 50 μM **1** was incubated with the cells and washed out with the loading buffer. Each data point represents the mean ± SEM, n = 4–12. *, ***, and n. s. mean $p < 0.05$, $p < 0.0005$, and not significant, respectively (unpaired t-test). (B) Representative $[Ca^{2+}]_i$ changes by 0.01 μM CAP after preincubation with 30 and 100 μM compound **1** in the HEK cells. Cell viability was checked by addition of 5 μM ionomycin. y-Axis: relative fluorescence unit (RFU). (C) Representative traces by superfusion of 0.1 μM CAP and 100 μM **1** to the rat DRG neurons. y-Axis: fluorescence intensity. (D) Example of the concentration–response curves for CAP in the absence and presence of 10, 30, 50, and 100 μM **1**. Data values for the compounds are each expressed as a percentage of the response to 10 μM CAP. Each data point represents the mean ± SEM, n = 4. (E) Mean result of Schild analysis of the antagonism produced by 10, 30, and 50 μM **1**. The slope and pA_2 value are calculated from six series of Schild plots. x-axis: voacangine (**1**) concentration (log M); y-axis: log (dose ratio − 1).

resiniferatoxin (RTX), CAP,[20] and cinnamaldehyde (CNA)[21] as naturally occurring antagonists. These are representative agonists at TRPV1 (RTX and CAP) and TRPA1 (CNA), and their TRPM8 blocking effect has been also reported. However, their inhibition mode against menthol and icilin on TRPM8 has not been identified.[20,21]

The calcium responses induced by 10 μM menthol and 0.3 μM icilin after the addition of each antagonist are shown in Figure 7A and C. All antagonists dose-dependently prevented menthol-induced activation. Meanwhile, most of the natural products scarcely attenuated icilin-induced activation, and only compound **1**, BCTC, and high concentrations of CAP showed inhibitory effects against icilin. When CPZ and each naturally occurring antagonist were administered at high concentrations (CPZ > 50 μM, RTX > 100 μM, CAP > 100 μM, and CNA > 500 μM), they caused strong nonspecific responses in the HEK cells. Accordingly, it was not possible to examine their TRPM8-blocking effect at higher concentrations. The IC_{50} values of the antagonists for menthol and icilin were calculated from dose–inhibition curves (for menthol, Figure 7B; for icilin, Figure 7D), and the values are shown in Table 1. The inhibitory potencies of **1** for both agonists were muchgreater than those of CPZ and the other naturally occurring antagonists. However, the IC_{50} values of **1** were 15 times greater (for menthol) and 25 times greater (for icilin) than those of BCTC.

Voacangine (1) Selectively Blocks Chemical Agonist-Induced Activation of TRPM8. The representative Ca^{2+} responses to cold with or without each antagonist in

dx.doi.org/10.1021/np400885u | J. Nat. Prod. 2014, 77, 285–297

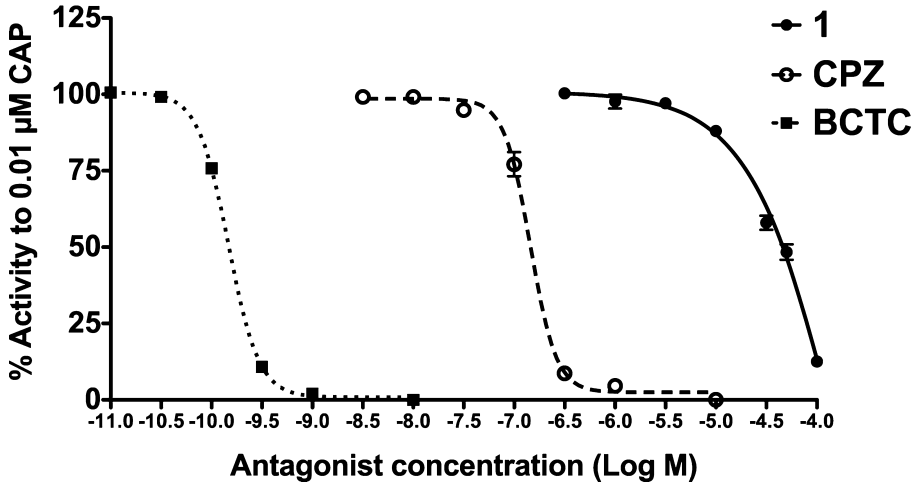

Figure 3. Determination of IC_{50} values of antagonists against TRPV1 activation by CAP. Fluo-4 responses by 0.01 μM CAP with pretreatment of 0.3−100 μM voacangine (**1**); 0.003−10 μM CPZ; and 0.00001−0.01 μM BCTC. Data for each compound are expressed as a percent response to 0.01 μM CAP. Each data point represents the mean ± SEM, n = 4−12.

Table 1. IC_{50} Values of the Antagonists on TRPV1 and TRPM8

	IC_{50} (μM)		
	TRPV1	TRPM8	
antagonist	0.01 μM CAP	10 μM menthol	0.3 μM icilin
voacangine (**1**)	50	9	7
BCTC	0.15 nM	0.35	0.4
CPZ	0.15	50	>50
RTX		>100	>100
CAP		28	>100
CNA		>500	>500

TRPM8-expressing HEK cells are shown in Figure 8. No Ca^{2+} response was observed in TREx HEK cells (not expressing TRPM8) when they were stimulated by cold (data not shown). When the cells were exposed to low-temperature perfusion buffer, Ca^{2+} influx was observed (Figure 8A), and it was blocked by addition of BCTC and CPZ (Figure 8C and D). On the contrary, compound **1** could not attenuate the response at all (Figure 8B and E).

Following the Ca^{2+} imaging, a patch-clamp analysis on the TRPM8-expressing HEK cells was performed. Figure 9A, C, and E are representative traces of the whole-cell current activated by 200 μM menthol, 200 μM icilin, and cold temperature in the presence and absence of 100 μM **1**. Compound **1** reversibly inhibited menthol- and icilin-induced activation (Figure 9A and C). In contrast, **1** had no effect on cold-induced activation (Figure 9E). These results are consistent with those of Ca^{2+} imaging, and thus both techniques showed chemical agonist-selective inhibition of **1** on TRPM8.

Compound **1** suppressed the chemical agonist-induced inward current to a stronger extent than the outward current. The antagonistic effect of **1** was voltage-dependent and was more effective in negative cell membrane voltage than in positive voltage (Figure 9B and D). When an antagonist acts in a competitive manner, that antagonist should not show voltage dependency. However, these results indicated a voltage-dependent blockade of **1** for both menthol and icilin. It may be possible that **1** exerts some effect on the voltage sensor region of TRPM8 (e.g., TM4, -5),[22] but the detailed mechanism remains to be clarified.

It was found that **1** is a competitive inhibitor of menthol and a stimulus-selective TRPM8 antagonist. To the best of our knowledge, no natural products that competitively inhibit the binding of menthol on TRPM8 have been reported; this is the first report of a stimulus-selective TRPM8 inhibitor.

All reports for point mutations of mTRPM8 indicate that Tyr745 situated in TM2 plays a critical role in menthol binding, and this mutant is unable to bind to radioactive menthol.[22] Icilin interacts with a wider pocket, including pivotal residues in TM3 (Asn799, Asp802, and Gly805) in rat TRPM8.[18] TRP box, TM4, and the TM4−5 linker have been implicated in cold sensing.[22,23] The present study showed that **1** competitively inhibited the binding of menthol and showed noncompetitive

Table 2. Agonistic and Antagonistic Activities of Voacangine (1) against Thermosensitive TRP Channels

TRP channel	effect	IC_{50} (μM)			mode of inhibition
TRPV1	antagonism	0.01 μM CAP 50	heat (45 °C) 24	proton (pH 5.9) no effect	competitive with CAP (K_B: 18 μM)
TRPM8	antagonism	10 μM menthol 9	0.3 μM icilin 7	cold (18 °C) no effect	competitive with menthol (K_B: 8.5 μM) noncompetitive with icilin
TRPA1	agonism	EC_{50} (μM) 8	TOP (%)[a] 98		

[a]% activity to 100 μM AITC.

dx.doi.org/10.1021/np400885u | J. Nat. Prod. 2014, 77, 285−297

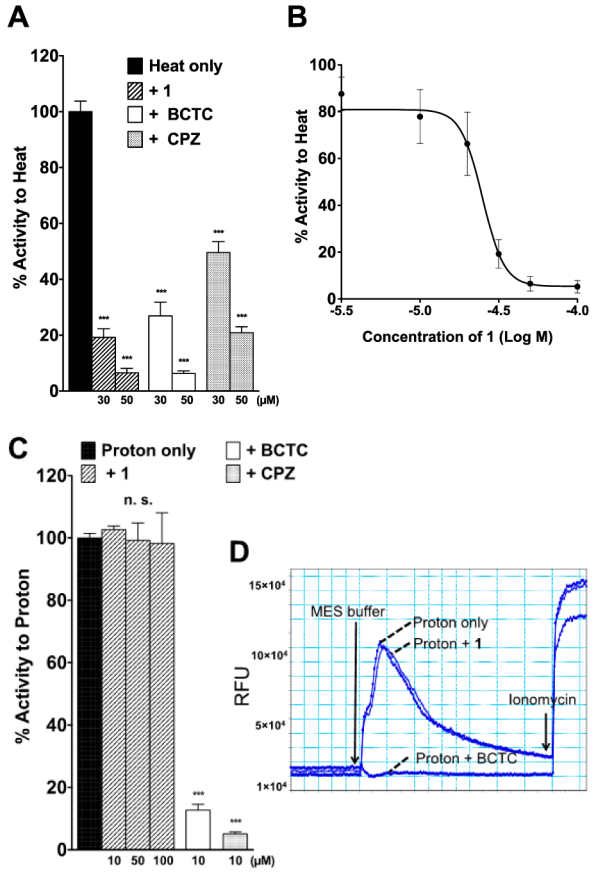

Figure 4. Effect of voacangine (**1**) against heat- and proton-evoked TRPV1 activation. Calcium response on TRPV1-expressing HEK cells induced by heat (A, B) and proton (C, D) is described. (A) Filled column, response by heat; other columns indicate heat-induced activation after treatment of each antagonist: slanted lined column, 30 and 50 μM **1**; white column, 30 and 50 μM BCTC; dotted column, 30 and 50 μM CPZ. (B) Calculation of IC_{50} value of **1** for heat-mediated TRPV1 activation. (C) Filled column, TRPV1 activation triggered by proton; other bars represent proton-evoked activation after antagonists were pretreated: slash striped column, 10, 50, and 100 μM compound **1**; unfilled column, 10 μM BCTC; dotted column, 10 μM CPZ. Data are expressed as percent responses to heat (A, B) and proton (C). Each data point represents the mean ± SEM, n = 4–10. *** and n. s. mean $p < 0.0005$ and not significant, respectively (unpaired t-test). (D) Fluorescence changes in the HEK cells when 100 μM **1** and 10 μM BCTC were incubated before addition of MES buffer (elicits proton-mediated TRPV1 activation).

inhibition against icilin but has no effect on cold-evoked activation. Accordingly, it was speculated that one of the binding sites of **1** may be Tyr745, which is a critical menthol binding site.

It was hoped to elucidate whether compound **1** binds to Tyr745 using a TRPM8 mutant. However, the Tyr745 mutant was insensitive not only to menthol but also to icilin, and it only responded to cold. Therefore, the inhibitory potencies of antagonists on Tyr745 mutant TRPM8 are able to be evaluated against cold-induced activation.[17,24] Unfortunately, compound **1** lacked inhibitory activity for cold, so its inhibitory effect on the mutant could not be examined.

Voacangine (1) Acts as an Agonist for TRPA1. The Ca^{2+} uptake in TRPA1-expressing HEK cells and TRPA1-non-expressing HEK cells (TREx HEK cells) is shown in Figure 10. Compound **1** showed a dose-dependent response on TRPA1-expressing cells. This response was significantly reduced by pretreatment with HC-030031, and compound **1** scarcely changed $[Ca^{2+}]_i$ on TRPA1-nonexpressing cells (Figure 10A). These results revealed that **1** is an agonist for TRPA1. The EC_{50} value for **1** was 8 μM, which was 15 times larger than that of AITC (EC_{50}: 0.5 μM). The maximal response of **1** was nearly equal to that of AITC (98%) (Figure 10B).

The original goals of this study were to measure the TRPV1 inhibitory effect of **1** using TRPV1-expressing cells and to examine the relationship between its TRPV1 blockade and the antidiarrheal activity of *V. africana*. It was found that compound **1** acted as an antagonist for TRPV1 and TRPM8 and as an agonist for TRPA1 at nearly equal concentrations (Table 2). TRPV1 and TRPA1 are expressed on sensory neurons innervating intestines. Although TRPM8 is found in sensory neurons of the human and mouse colon,[25] its expression in the stomach and small intestine in rodents remains controversial.[26] A number of reports have indicated that TRPV1 is relevant to various gastrointestinal disorders (e.g., irritable bowel syndrome, inflammatory bowel disease, colitis, abdominal pain, and fecal urgency). Furthermore, recent studies have reported that TRPV1 antagonists (CPZ and JNJ 10185734) can alleviate pain and discomfort in rodents with colitis.[27] There is substantial evidence that TRPA1 participates in inflammation-evoked mechanical and chemical hypersensitivity in the digestive system. Furthermore, it has been indicated that activation of TRPA1 in enterochromaffin cells promotes gastrointestinal contractions by inducing serotonin secretion.[28] For TRPM8, previous studies have suggested that it may play a chemosensory role in the alimentary canal. A recent report has suggested that icilin attenuates chemically induced colitis and indicates an anti-inflammatory role for TRPM8.[25] However, systematic studies of the chemosensory role of TRPM8-expressing primary afferent neurons in the gut have not been reported, and the precise functional implications of TRPM8 in the digestive system await future studies. Association of TRPV1 with abdominal pain and diarrhea has been implicated, and TRPA1 agonists can facilitate contraction of the gastrointestinal tract. Currently, the physiological functions of TRPM8 in the gastrointestinal tract are mostly unknown. At present, it is difficult to speculate how **1** may affect the human alimentary canal though activation and inhibition of TRP channels.

Recent reports show that TRPM8 is involved in cold allodynia and cold hypersensitivity following nerve injury, and pain in urological disorders. Therefore, TRPM8-blocking drugs are being widely developed as a potential new therapy for these pain disorders.[29] Among TRP channel inhibitors, TRPV1 blockers for analgesic treatment have been the most developed. However, their side effects (elevation of core body temperature and impairment of thermal sensation) prevent their practical use.[30] The mechanism underlying TRPV1 antagonist-mediated hyperthermia is not clear, but several strategies have been proposed to overcome these side effects.[31] One of them is to develop stimulus-specific TRPV1 blockers. Recent reports have suggested that stimulus-specific TRPV1 antagonists that selectively inhibit CAP and heat are devoid of a hyperthermic effect.[32,33] Highly selective TRPM8 antagonists have been reported to cause decrease in the core temperature and reduction in cold avoidance in rodents.[34] When the developmental history of TRPV1-blocking drugs is considered, it is important to find TRPM8 antagonists having diverse chemical structures and stimulus-selectivity for developing TRPM8 blockers without any side effects. It has been also

dx.doi.org/10.1021/np400885u | J. Nat. Prod. 2014, 77, 285–297

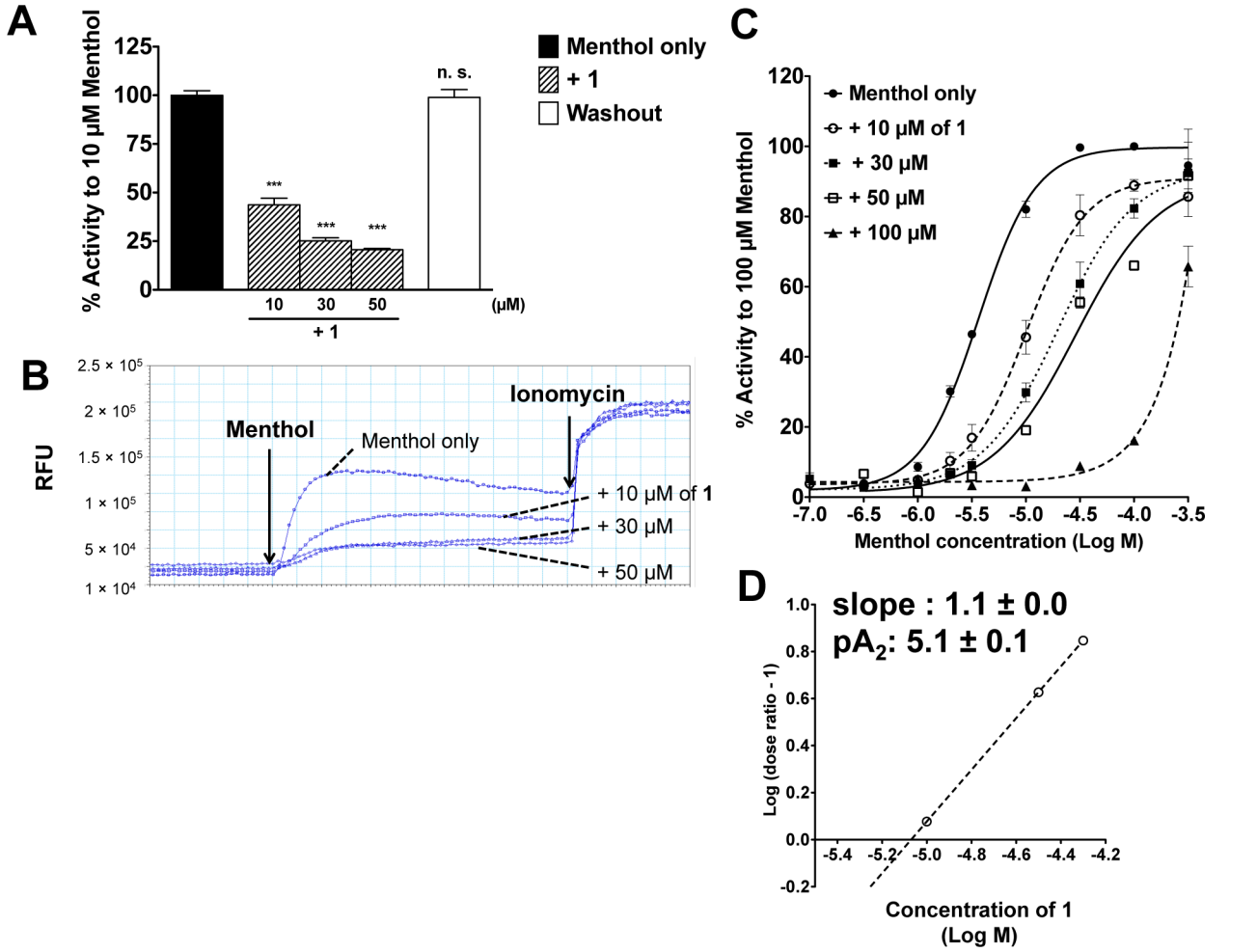

Figure 5. Antagonistic activity of voacangine (**1**) against menthol-evoked TRPM8 activation. $[Ca^{2+}]_i$ change on TRPM8-expressing HEK cells (A, B, C) and Schild plot (D) are displayed. (A) Filled column, TRPM8 activation evoked by 10 μM menthol; oblique lined column, menthol-induced activation when the cells were preincubated with 10, 30, and 50 μM **1**; white column, response by 10 μM menthol after addition of 50 μM **1** and washout treatment was performed. (B) Representative chart of Ca^{2+} influx triggered by 10 μM menthol after pretreatment of HEK cells with 10, 30, and 50 μM **1**. *y*-Axis: relative fluorescence unit (RFU). (C) Dose−response relationships of 0.1−300 μM menthol in the presence and absence of 10, 30, 50, and 100 μM **1**. (D) Mean result of the Schild plot obtained by 10, 30, and 50 μM compound **1**-induced TRPM8 inhibition. The slope and pA_2 value were calculated from five series of Schild plots. *x*-Axis: voacangine (**1**) concentration (log M); *y*-axis: log (dose ratio − 1) (D). On graphs A and C, each data point represents the mean ± SEM, n = 4−12. Data are expressed as percent responses to 10 μM menthol (A) and 100 μM menthol (C). *** represents $p < 0.0005$, and n. s. indicates not significant (unpaired *t*-test).

shown that **1** competes with menthol on TRPM8. There have been no reports that examine relationships between binding sites of TRPM8 antagonists and their therapeutic potential or side effects. Thus, it is not clear what type of antagonist having binding sites is best for TRPM8-blocking drugs. However, it would be important to identify TRPM8 inhibitors having different binding sites to develop side-effect-free TRPM8 blockers. Although the selectivity of **1** for thermosensitive TRPs is not high, it showed a unique TRPM8 inhibitory effect through its stimulus-selective inhibition. Therefore, this may contribute to the development of a new class of stimulus-selective TRPM8 inhibitors.

EXPERIMENTAL SECTION

Materials. Voacangine (**1**) was purified from the root bark of *V. africana* (purity: more than 97.5% by 600 MHz NMR spectrum).[13]

Capsaicin (CAP), capsazepine (CPZ), L-α-lysophosphatidylcholine (LPC) from *Glycine max* (soybean), ruthenium red (RR), cinnamaldehyde (CNA), and resiniferatoxin (RTX) were purchased from Sigma-Aldrich (St. Louis, MO, USA). Allyl isothiocyanate (AITC) and (−)-menthol were obtained from Wako Pure Chemical Industries (Osaka, Japan). HC-030031 was obtained from ChemBridge (San Diego, CA, USA). 4-(3-Chloro-2-pyridinyl)-*N*-[4-(1,1-dimethylethyl)phenyl]-1-piperazinecarboxamide (BCTC) was obtained from Tocris BioScience (Bristol, UK).

TRP Channel-Expressing HEK Cells. Human TRPV1 (hTRPV1), hTRPA1, and mouse TRPM8 (mTRPM8) were stably expressed in HEK293T cells (TRPV1) or HEK T-REx cells (TRPA1 and TRPM8). hTRPV2 and hTRPV3 were transiently expressed in HEK293T cells. hTRPV1, hTRPA1, and mTRPM8 cDNA was amplified by RT-PCR from first-strand cDNA from human brain (hTRPV1) (Agilent Technologies, Santa Clara, CA, USA), human WI38 cells (hTRPA1), and mouse dorsal root ganglion cells (mTRPM8). The following primers were used for cloning: TRPV1 forward primer 5′-GCAAGGATGAAGAAGAAATGGA-3′ and reverse primer 5′-TCACTTCTCCCCGGAAGCGC-3′; TRPA1 forward primer 5′-TGGGTCAATGAAGTGCAG-3′ and reverse primer 5′-GAAGGTCTGAGGAGCTAAGGC-3′; mTRPM8 forward primer 5′- ATGTCCTTCGAGGGAGCCAG-3′ and reverse primer 5′-CGCCAGCCTTACTTGATGTT-3′. hTRPV2 (SKU: SC320356) and hTRPV3 (SKU: SC316997) were purchased from Origene (Rockville, MD, USA). Except for TRPV1 cDNA, the cDNA for the

dx.doi.org/10.1021/np400885u | J. Nat. Prod. 2014, 77, 285−297

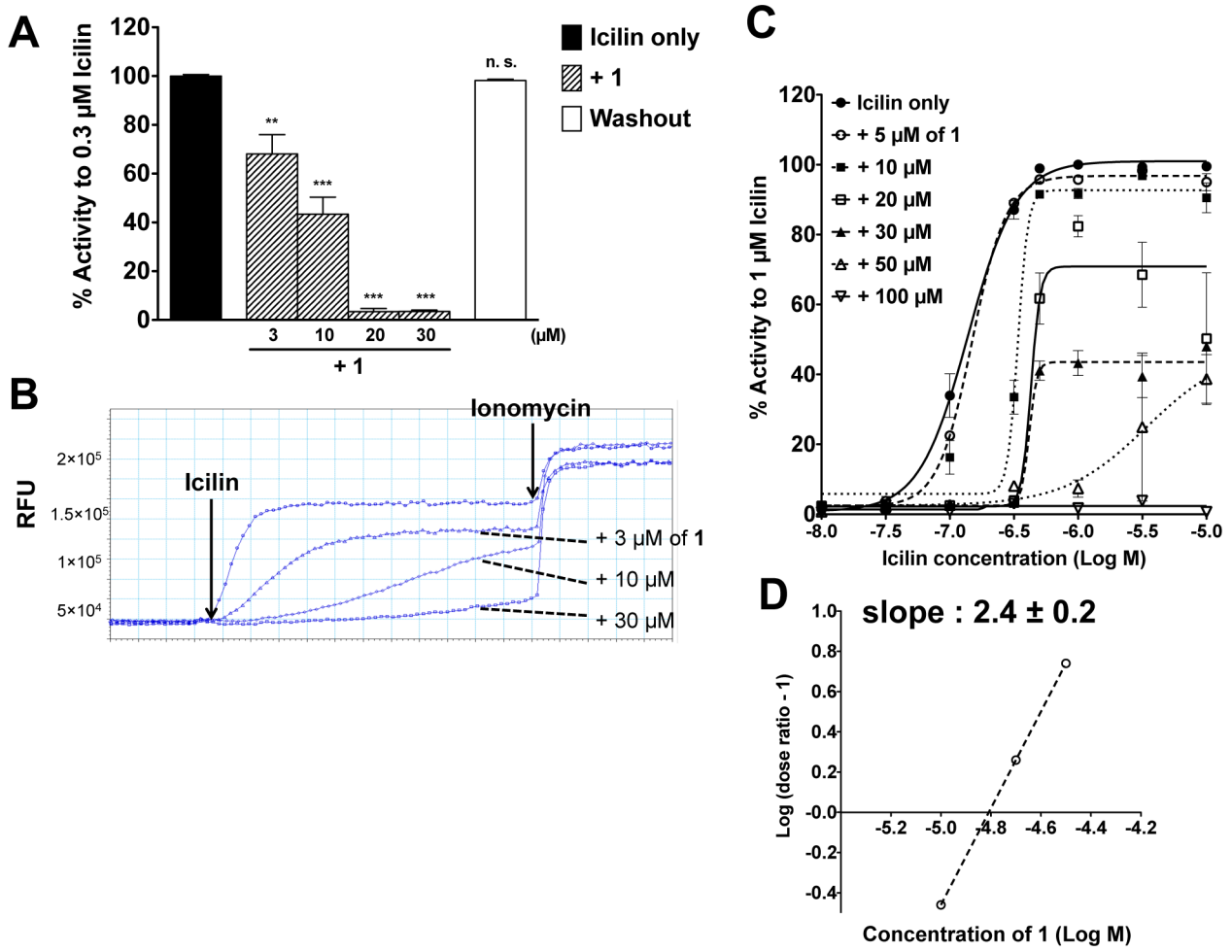

Figure 6. (A) Abrogation of icilin-induced TRPM8 activation by addition of voacangine (**1**). Ca^{2+} uptake in the TRPM8-expressing HEK cells evoked by icilin in the absence and presence of **1**. Solid column, response produced by 0.3 μM icilin; slash striped column, TRPM8 activity of icilin after addition of 3, 10, 20, 30 μM **1**; open column, response by icilin after treatment of 100 μM **1** and washout of the cells. (B) Representative fluorescence change elicited by 0.3 μM icilin with preincubation of the HEK cells with 3, 10, and 30 μM **1**. *y*-Axis: relative fluorescence unit (RFU). (C) Example of the dose−response curves for icilin in the absence and presence of 5, 10, 20, 30, 50, and 100 μM **1**. (D) Mean result of Schild analysis of the antagonism produced by 10, 20, and 30 μM **1**. The slope and pA_2 value are calculated from five sets of Schild plot analyses. *x*-Axis: voacangine (**1**) concentration (log M); *y*-axis: log (dose ratio − 1). On graphs A and C, each data point represents the mean ± SEM, $n = 4–12$. Data values are expressed as a percent response to 0.3 μM icilin (A) and 1 μM icilin (C). *** represents $p < 0.0005$, and n. s. indicates not significant (unpaired *t*-test).

channels was subcloned into pcDNA4/TO (Invitrogen, Carlsbad, CA, USA). TRPV1 cDNA was subcloned into pcDNA3 (Invitrogen) and then transfected into HEK293T cells using SuperFect transfection reagent (Qiagen, Hilden, Germany). After culturing cells in the presence of 750 μg/mL G418, a HEK293T cell line was obtained that stably expressed TRPV1. The stable expression of full-length TRPA1 or TRPM8 in HEK T-REx cells was induced using the tetracycline-inducible T-REx expression system (Invitrogen). The plasmids were transfected into HEK T-REx cells by using Lipofectamine 2000 reagent (Invitrogen). HEK T-REx cells stably maintaining the TRPA1 or TRPM8 gene were selected using 500 μg/mL zeocin and 10 μg/mL blasticidin and grown according to the manufacturer's instructions. hTRPV2 or hTRPV3 plasmids were transiently transfected into HEK293T cells using Lipofectamine LTX reagent (Invitrogen).

The HEK cells were cultured in Dulbecco's modified Eagle medium (Wako Pure Chemical Industries, Ltd.) with 10% fetal bovine serum (FBS) (Wako), 100 unit/mL penicillin, 100 mg/mL streptomycin, and 250 ng/mL amphotericin (Nacalai Tesque, Kyoto, Japan). The cells were subcultured every week, and the highest passage number was 40.

Primary Culture of Rat DRG Neurons. DRG neurons were dissected from 4-week-old Wistar rats. The extirpated DRG neurons were dissociated by incubation for 1 h in MEM-complete (Earl's balanced salt solution [Sigma] containing 5% FBS, 100 unit/mL penicillin, 100 μg/mL streptomycin, 250 ng/mL amphotericin B [Nacalai Tesque], 2 mM L-alanyl-L-glutamine [Gibco], and 1× MEM vitamin solution [Sigma]) with 125 mg/mL collagenase P solution (Roche, Basel, Switzerland). Thereafter, the neurons were triturated and cultured in MEM complete with 10 μg/mL nerve growth factor (NGF-7S, Sigma) on polylysine-coated 96-well plates 24−36 h before the assay.

The animal experiments were approved by the Animal Care and Use Committee of the University of Shizuoka (protocol number 135020). When the DRG neurons were isolated from the rodents, they were anesthetized to minimize the pain.

Measurement of Intracellular Ca^{2+} Concentration. The intracellular Ca^{2+} concentration ($[Ca^{2+}]_i$) was measured using a FlexStation II system (Molecular Devices, Sunnyvale, CA, USA) at 37 °C. The TRPV1-, TRPA1-, or TRPM8- expressing cells were seeded in 96-well plates 24 h before the assay. To obtain TRPA1- or TRPM8-expressing HEK cells, 1 μg/mL tetracycline was added to induce the expression of these TRP channels. TRPV2- or TRPV3-expressing cells were seeded in 96-well plates 6 h after transfection and incubated for 18 h at 37 °C before calcium imaging. The HEK cells were loaded with 3 μM Fluo-4 AM (Dojindo Laboratories, Kumamoto, Japan) for 1 h at

dx.doi.org/10.1021/np400885u | J. Nat. Prod. 2014, 77, 285−297

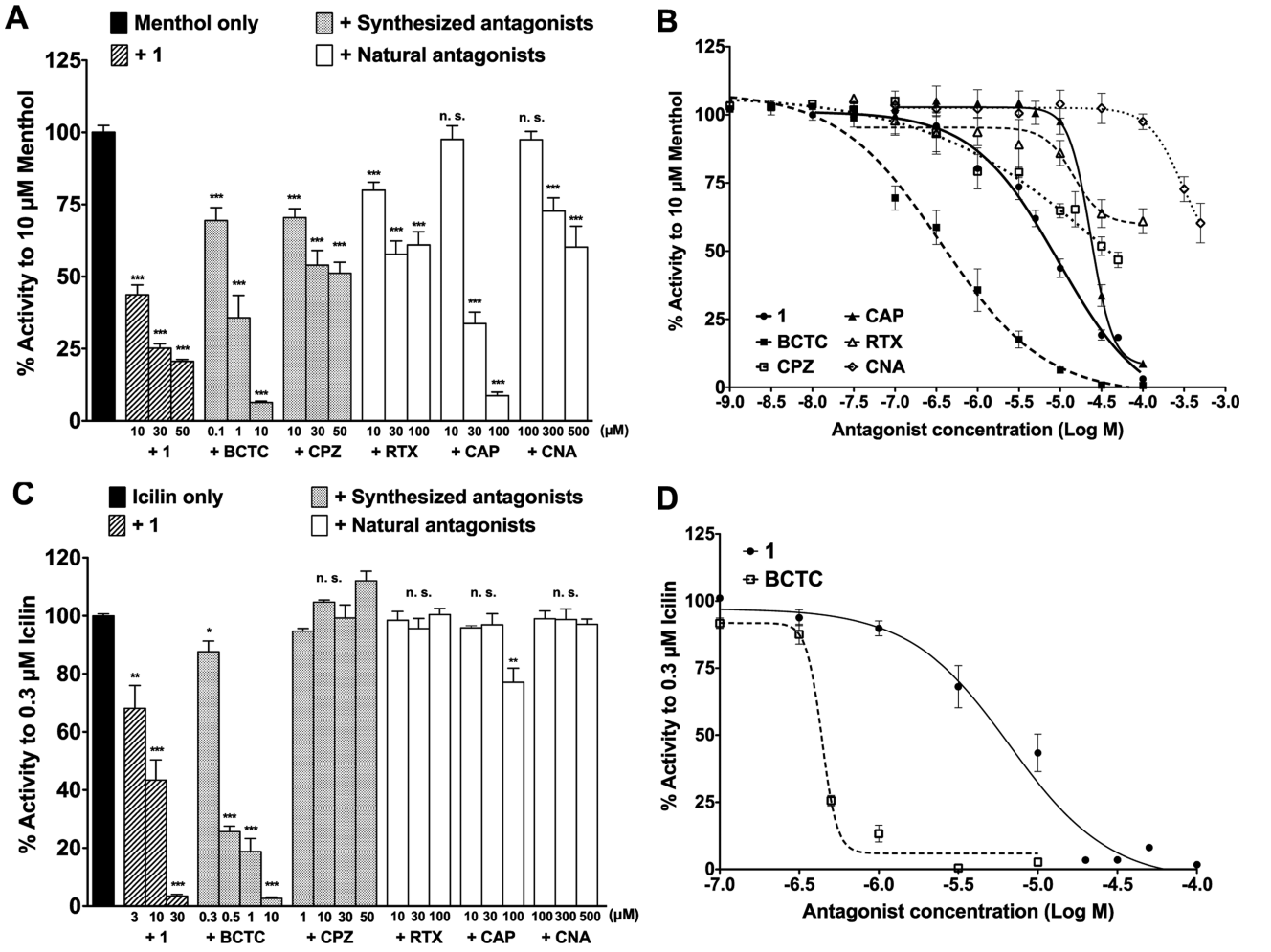

Figure 7. Comparison of TRPM8 inhibitory potency of voacangine (**1**) with known antagonists. Fluo-4 response induced by menthol (A, B) and icilin (C, D) in the presence and absence of TRPM8 antagonists on the TRPM8-expressing HEK cells. (A) Filled column, activity of 10 μM menthol; other columns show responses produced by 10 μM menthol after treatment with following antagonists: hatched column, 10, 30, and 50 μM **1**; dotted column, synthetic antagonists (0.1, 1, and 10 μM BCTC and 10, 30, and 50 μM CPZ); unfilled column, natural antagonists (10, 30, and 100 μM RTX and CAP, 100, 300, and 500 μM CNA). (B) Determination of IC_{50} values of the antagonists against 10 μM menthol-evoked activation. Concentrations of 0.01−100 μM **1**, 0.001−100 μM BCTC, 0.001−50 μM CPZ, 0.03−100 μM RTX, 0.1−100 μM CAP, and 0.1−500 μM CNA were added to the cells before addition of 10 μM menthol. (C) Filled column, activation by 0.3 μM icilin; other columns indicate activity of 0.3 μM icilin with preincubation with the following antagonists: slanted line column, 3, 10, and 30 μM of **1**; dotted column, synthetic antagonists (0.3, 0.5, 1, and 10 μM BCTC and 1, 10, 30, and 50 μM CPZ); open column, natural antagonists (10, 30, and 100 μM RTX and CAP, 100, 300, and 500 μM CNA). (D) Comparison of IC_{50} values of voacangine (**1**) with that of BCTC against 0.3 μM icilin-induced activation. Cells with treated with 0.1−100 μM **1** and 0.1−10 μM BCTC before addition of 0.3 μM icilin. Each data point represents the mean ± SEM, n = 4−12. Data are expressed as percent responses to 10 μM menthol (A, B) and 0.3 μM icilin (C, D). * represents $p < 0.05$, *** indicates $p < 0.0005$, and n. s. indicates not significant (unpaired t-test).

37 °C in a normal loading buffer (measuring buffer) containing 5.37 mM KCl, 0.44 mM KH_2PO_4, 137 mM NaCl, 0.34 mM $Na_2HPO_4 \cdot 7H_2O$, 5.56 mM D-glucose, 20 mM HEPES, 1 mM $CaCl_2$, 0.1% BSA, and 2.5 mM probenecid (pH 7.4). Probenecid is an agonist for TRPV2, so probenecid-free buffer was used for TRPV2. When measuring TRPV3 activity, the temperature for the assay and the loading was set at 25 °C.

For measuring cold-induced TRPM8 activation of the HEK cells, a perfusion system was used along with a fluorescence microscope (AF6000, Leica Microsystems, Wetzlar, Germany). The cells were seeded on cover glasses (3 × 10 mm, Matsunami Glass, Osaka, Japan) and incubated at 37 °C in 5% CO_2, 24 h before the assay. The cells were loaded with 3 μM Quest Fluo-8 AM (AAT Bioquest, Sunnyvale, CA, USA) for 1 h at 37 °C in the measuring buffer. Data were sampled using LAS AF software (Leica Microsystems). All experiments were performed at room temperature.

All of the compounds were used at a concentration at which they did not show a nonselective effect on HEK cells not expressing TRP channels (HEK293T cells or HEK T-REx cells). The test compounds were dissolved in dimethyl sulfoxide (DMSO) and added to the loading solution. The final concentration of DMSO was 0.1−0.3% for TRPA1, TRPM8, TRPV2, and TRPV3 and 0.1−1% for TRPV1. LPC was dissolved in methanol, and its final concentration was 0.1% for TRPV3. These solvents did not affect HEK cells at the above concentrations.

After activation of the TRP channels, 5 μM ionomycin (in a FlexStation II system) or 50 μM ionomycin (in a fluorescence microscope using a perfusion system) was added to the cells. Ionomycin was used to check the cell variability and to get the maximum fluorescence intensity of cells. The data values for the test compounds except for TRPV2 were expressed as a percentage of the response to 5 μM ionomycin. The calcium responses of TRPV2 were smaller than those of the other TRP channels. Therefore, the

dx.doi.org/10.1021/np400885u | J. Nat. Prod. 2014, 77, 285−297

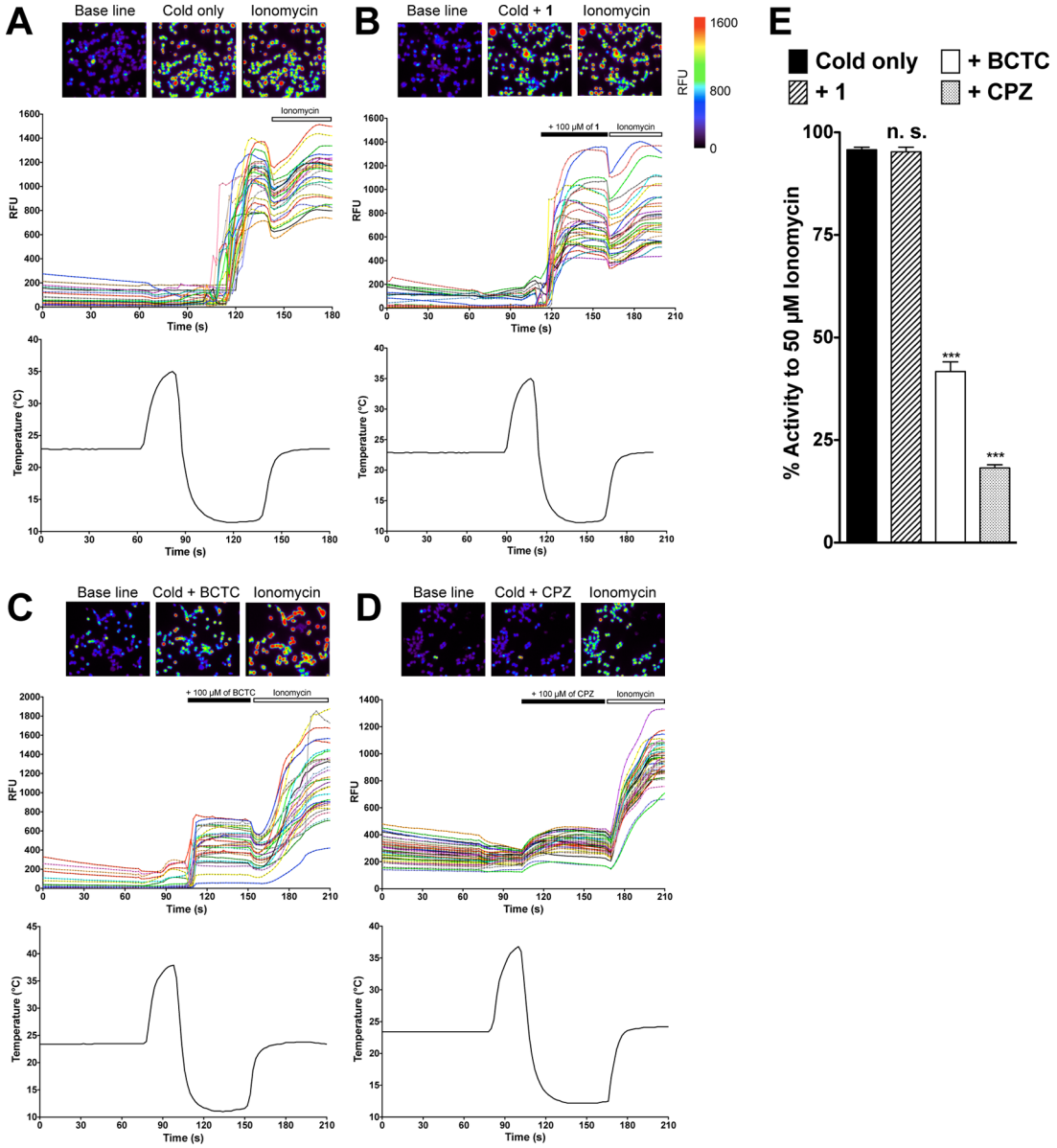

Figure 8. Influence of voacangine (**1**) on TRPM8 activation by a cold temperature. Cold-induced Ca^{2+} uptake in TRPM8-expressing HEK cells in the absence (A) and the presence of 100 μM **1** (B), BCTC (C), and CPZ (D). Representative fluorescence images (upper), traces from individual cells (middle), and temperature changes of perfusion buffer (lower) are shown. The pseudocolor indicates fluorescence intensity of excitation at 480 nm and emission at 527 nm. Horizontal bars indicate the duration of compound application. (E) Cold-induced responses in individual cells with each antagonist. Filled column, response by cold; other columns indicate cold-induced activation when the following antagonists (100 μM) were applied: hatched column, **1**; open column, BCTC; dotted column, CPZ. Data are expressed as percent responses to 50 μM ionomycin. Each data point represents the mean ± SEM, n = 32−39. *** and n. s. mean $p < 0.0005$ and not significant, respectively (unpaired t-test).

responses obtained (F) were normalized to the fluorescence at baseline (F_0) and expressed as the $\Delta F/F_0$ value (%): $\Delta F/F_0$ (%) = $(F - F_0)/F_0 \times 100$. Curve fitting and parameter estimation were performed using Prism 5a software (Graph Pad Software, San Diego, CA, USA).

Functional Assays by Ca^{2+} Imaging. Owing to the low water solubility, voacangine (**1**) was used at less than 100 μM in all experiments. In the case of the Schild plots, **1** was utilized at concentrations of 10−50 μM. All of the antagonists were preincubated with the cells in the measuring buffer at 37 °C for 3 min prior to addition of each concentration of the agonists.

Agonist and Antagonist Assay on Thermo-TRPs. The following agonists were used as positive controls for each TRP channel: 10 μM CAP for TRPV1; 100 μM menthol and 1 μM icilin for TRPM8; 100 μM AITC for TRPA1; 40 μM LPC for TRPV2; 1000 μM menthol for TRPV3. For antagonism experiments, the following agonists and antagonists were administered: 0.01 μM CAP and 10 μM BCTC for TRPV1; 10 μM menthol, 0.3 μM icilin, and 10 μM BCTC for TRPM8; 3 μM AITC and 30 μM HC-030031 for TRPA1; 30 and 40 μM LPC and 5 μM RR for TRPV2; 100 and 300 μM menthol and 5 μM RR for TRPV3.

Antagonist Assay on TRPV1 Heating. The cell plates were heated from 40 to 45 °C using the FlexStation II system to activate TRPV1 by heat, and the Ca^{2+} signal measurement was performed for 42 min.

Proton-Mediated Activation. For the measurement of proton-mediated activation of TRPV1, 2-morpholinoethanesulfonic acid monohydrate (MES) buffer (5.37 mM KCl, 0.44 mM KH_2PO_4, 137 mM NaCl, 0.34 mM $Na_2HPO_4{\cdot}7H_2O$, 5.56 mM D-glucose, 20 mM MES, and 1 mM $CaCl_2$ at pH 4.0) was used. The MES buffer was added to measuring buffer (pH 7.4) in the cell plates using the

dx.doi.org/10.1021/np400885u | J. Nat. Prod. 2014, 77, 285−297

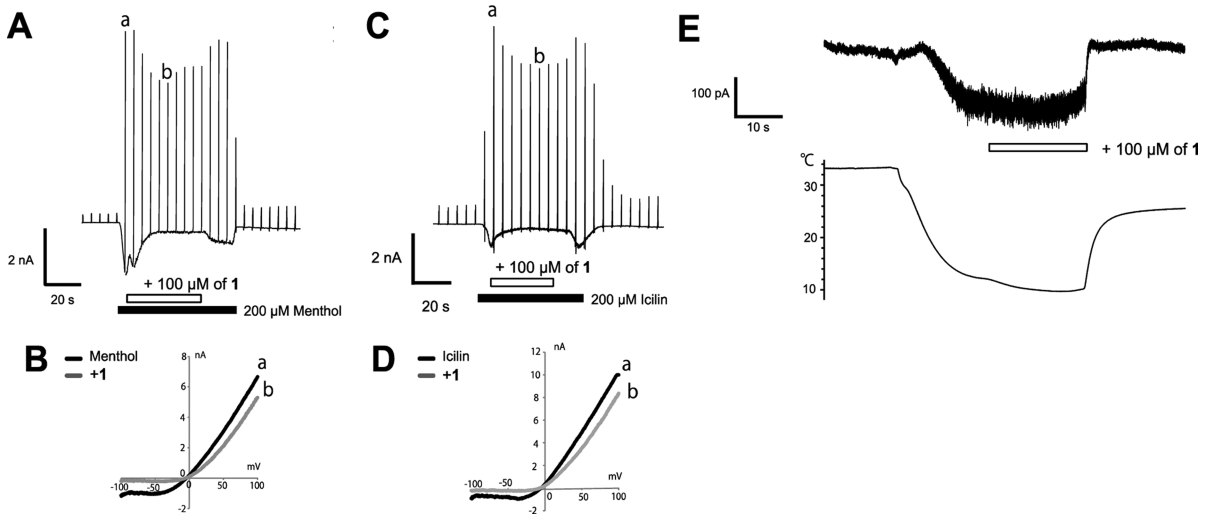

Figure 9. Stimulus-selective blockade of voacangine (**1**) against TRPM8 activation by chemical agonists and cold. Representative traces of whole-cell current activated by 200 μM menthol (A), 200 μM icilin (C), and cold (E) in the absence and presence of 100 μM compound **1** in TRPM8-expressing HEK cells. Holding potential (Vh), −60 mV. (A, C, E) Horizontal bars indicate the duration of compound application. Representative *I*–*V* curves of current induced by 200 μM menthol (B) and 200 μM icilin (D) with or without 100 μM **1**.

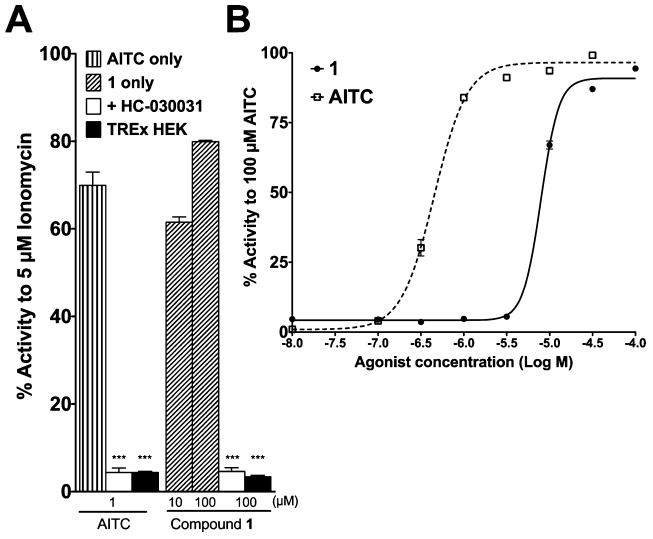

Figure 10. Agonistic effect of voacangine (**1**) on TRPA1. TRPA1-mediated Ca^{2+} uptake in TRPA1-expressing HEK cells evoked by AITC and compound **1**. (A) Lined column, activation by 1 μM AITC and 10 and 100 μM **1**; unshaded column, response by 1 μM AITC and 100 μM of **1** in the presence of 30 μM HC-030031; shaded column, response by the above concentrations of AITC and **1** in TREx-HEK cells not expressing TRPA1. (B) Dose–response curves by AITC and compound **1**. AITC and **1** (0.01–100 μM) were administered to the cells. Each data point represents the mean ± SEM, n = 4–8. Data values are expressed as a percent response to 5 μM ionomycin (A) and 100 μM AITC (B). *** indicates $p < 0.0005$ (unpaired t-test).

FlexStation II system, and the pH of the measuring buffer was equilibrated to about 5.9.

Antagonist Assay on TRPM8: Chemical Agonists. Concentrations of 0.1–10 μM BCTC, 1–50 μM CPZ, 10–100 μM RTX and CAP, and 100–500 μM CNA were used to examine their suppressive effect against menthol and icilin. When IC_{50} values of the antagonists were determined, they were administered at the following concentrations: for menthol, 0.01–100 μM **1**, 0.01–50 μM CPZ, 0.001–100 μM BCTC, 0.03–100 μM RTX, 0.1–100 μM CAP, and 1–500 μM CNA; for icilin, 0.1–100 μM **1** and 0.1–10 μM BCTC.

Cold. Coverslip pieces with cultured HEK cells were placed in a microchamber (Warner Instruments, LLC, Hamden, CT, USA) and continuously perfused with the measuring buffer that was maintained at room temperature (approximately 23–24 °C). To evoke cold-induced TRPM8 activation, the buffer of following temperatures was perfused: 23–24 °C, 35–37 °C, and 11–12 °C (containing 100 μM antagonist). Temperature was monitored with a thermocouple probe (SE61308, Anritsu Meter Co., Ltd., Tokyo, Japan).

Washout Experiment. A washout experiment was performed to examine whether the **1**-induced inhibition of TRPV1 was reversible. The TRP channel-expressing HEK cells, which were incubated with 50 μM **1** for 3 min, were washed six times with the measuring buffer. After this, the cells were left for 10 min at 37 °C in the dark, followed by treatment with each agonist (0.01 μM CAP for TRPV1, 10 μM menthol and 0.3 μM icilin for TRPM8).

Schild Plot Analysis (ref 35). The Schild equation was applied for analysis of the inhibition mode of the antagonists. For instance, TRPV1 antagonists, such as BCTC, SB-366791, A-784168, and A-795614, have been demonstrated for their CAP competitive inhibition using the Schild equation.[36−38] The most important application of the Schild equation is that it provides a way of estimating pA_2 and K_B values. As defined, pA_2 is an empirical index of the action of an antagonist, and it is the negative log of K_B, while K_B is the equilibrium dissociation constant for the combination of an antagonist with its binding site. When the antagonism is competitive, the intercept of a Schild plot on the abscissa yields an estimate of pA_2 (negative log of K_B).

In this study, the Schild equation was applied to investigate the inhibition mode of voacangine (**1**) against each TRPV1 and TRPM8 agonist. Dose–response curves for one series of agonists in the presence and absence of each concentration of antagonist gave one series of Schild plots. In the Schild plot, a competitive antagonist gives a straight line and its slope represents unity (1.0). However, if the slope of the Schild plot differs significantly from unity, the antagonism is noncompetitive. To estimate the exact slope of the Schild plot, five or six series of dose–response curves and Schild plots were obtained. Statistical analysis was performed to examine whether their slopes differed significantly from unity (paired t-test). When the slopes did not differ significantly from unity, the antagonism was regarded as competitive, and if they did, the antagonism was noncompetitive.

Whole-Cell Patch-Clamp Recording. HEK293 cells were maintained in DMEM (Wako) containing 10% fetal bovine serum (Biowest SAS, Caille, France), 100 units/mL penicillin (Invitrogen), 100 μg/mL streptomycin (Invitrogen), and 2 mM GlutaMAX

(Invitrogen) at 37 °C in 5% CO_2. A 1 μg quantity of mTRPM8 (donated by Dr. Ardem Patapoutian) in pcDNA3 and 0.1 μg of pGreen Lantern 1 expression cDNA were transfected to the HEK cells using OPTI-MEM medium (Invitrogen) and Lipofectamine Plus reagent (Invitrogen). After incubating for 3−4 h, cells were reseeded on coverslips and further incubated at 37 °C in 5% CO_2. Whole-cell patch-clamp recordings were performed 1 day after transfection. HEK293 cells on coverslips were mounted in an open chamber (Warner Instruments, LLC) and perfused with standard bath solution (140 mM NaCl, 5 mM KCl, 2 mM $MgCl_2$, 2 mM $CaCl_2$, 10 mM HEPES, 10 mM glucose, pH 7.4). Composition of the pipet solution is 140 mM KCl, 5 mM EGTA, and 10 mM HEPES, pH 7.4 (with KOH). Data were sampled at 10 kHz and filtered at 5 kHz for analysis (Axon 200B amplifier with pCLAMP software, Axon Instruments). The membrane potential was clamped at −60 mV, and voltage ramp-pulses from −100 to +100 mV (500 ms) were applied every 5 s. All experiments were performed at room temperature. To trigger cold-induced activation, cells were exposed in the following order to temperature-controlled buffer: 25 °C, 32−35 °C, and 10 °C. When examining the inhibitory potency of voacangine (**1**), 100 μM containing buffer at 10 °C was superfused. Temperature was monitored with a thermocouple (TA-29, Warner Instruments) placed within 100 μm of the patch-clamped cell.

AUTHOR INFORMATION

Corresponding Author

*Tel: +81-054-264-5543. Fax: +81-054-264-5550. E-mail: watanbt@u-shizuoka-ken.ac.jp.

Notes

The authors declare no competing financial interest.

ACKNOWLEDGMENTS

This study was supported in part by the Grants-in-Aid for Scientific Research from JSPS (2410919 to Y.T. and 24580194 to T.W.). This study was supported by the Cooperative Study Program of National Institute for Physiological Sciences.

REFERENCES

(1) Bouquet, A.; Debray, M. In *Plant Medicinals de la Cote d'Ivoire*; Office de la Recherche Scientifique et Technique d'Outre Mer (ORSTOM): Paris, 1974; Vol. *165*, 11, pp 38−39.

(2) Adjanohoun, J. E.; Aboubakar, N.; Dramane, K.; Ebot, M. E.; Ekpere, J. A.; Enow-Orock, E. G.; Focho, D.; Gbile, Z. O.; Kamanyi, A.; Kamsu-Kom, J.; Keita, A.; Mbenkum, T.; Mbi, C. N.; Mbiele, A. L.; Mbome, L. L.; Mubiru, N. K.; Nancy, W. L.; Nkongmeneck, B.; Satabie, B.; Sofowara, A.; Tamze, V.; Wirmum, C. K. In *Traditional Medicine and Pharmacopoeia: Contribution to Ethnobotanical and Florisic Studies in Cameroon*; Organization of Africa Unity Scientific, Technical and Research Commision (OUA/STRC), Centre Nationale de Production de Mauels Scolaires: Porto-Novo, Benin, 1996; p 63.

(3) Tan, P. V.; Njimi, C. K.; Ayafor, J. F. *Phytother. Res.* **1997**, *11*, 45−47.

(4) Tan, P. V.; Penlap, V. B.; Nysse, B.; Nguemo, J. D. B. *J. Ethnopharmacol.* **2000**, *73*, 423−428.

(5) Caterina, M. J.; Schumacher, M. A.; Tominaga, M.; Rosen, T. A.; Levine, J. D.; Julius, D. *Nature* **1997**, *389*, 816−824.

(6) Tominaga, M.; Caterina, M. J.; Malmberg, A. B.; Rosen, T. A.; Gilbert, H.; Skinner, K.; Raumann, B. E.; Basbaum, A. I.; Julius, D. *Neuron* **1998**, *21*, 531−543.

(7) Patterson, L. M.; Zheng, H.; Ward, S. M.; Berthoud, H. R. *Cell Tissue Res.* **2003**, *311*, 277−287.

(8) Ward, S. M.; Bayguinov, J.; Won, K. J.; Grundy, D.; Berthoud, H. R. *J. Comp. Neurol.* **2003**, *465*, 121−135.

(9) Cortright, D. N.; Szallasi, A. *Eur. J. Biochem.* **2004**, *271*, 1814−1819.

(10) Holzer, P. *Gastroenterology* **1998**, *114*, 823−839.

(11) Holzer, P. *Auton. Neurosci.* **2006**, *125*, 70−75.

(12) Bartho, L.; Benko, R.; Patacchini, R.; Petho, G.; Holzer-Petsche, U.; Holzer, P.; Lazar, Z.; Undi, S.; Illenyi, L.; Antal, A.; Horvath, O. P. *Eur. J. Pharmacol.* **2004**, *500*, 143−157.

(13) Lo, M. W.; Matsumoto, K.; Iwai, M.; Tashima, K.; Kitajima, M.; Horie, S.; Takayama, H. *J. Nat. Med.* **2011**, *65*, 157−165.

(14) Gavva, N. R.; Klionsky, L.; Qu, Y.; Shi, L.; Tamir, R.; Edenson, S.; Zhang, T. J.; Viswanadhan, V. N.; Toth, A.; Pearce, L. V.; Vanderah, T. W.; Porreca, F.; Blumberg, P. M.; Lile, J.; Sun, Y.; Wild, K.; Louis, J. C.; Treanor, J. J. *J. Biol. Chem.* **2004**, *279*, 20283−20295.

(15) Tominaga, M.; Tominaga, T. *Pflugers Arch.* **2005**, *451*, 143−150.

(16) Khairatkar-Joshi, N.; Szallasi, A. *Trends Mol. Med.* **2009**, *15*, 14−22.

(17) Bandell, M.; Dubin, A. E.; Petrus, M. J.; Orth, A.; Mathur, J.; Hwang, S. W.; Patapoutian, A. *Nat. Neurosci.* **2006**, *9*, 493−500.

(18) Chuang, H. H.; Neuhausser, W. M.; Julius, D. *Neuron* **2004**, *43*, 859−869.

(19) Malkia, A.; Morenilla-Palao, C.; Viana, F. *Curr. Pharm. Biotechnol.* **2011**, *12*, 54−67.

(20) De Petrocellis, L.; Starowicz, K.; Moriello, A. S.; Vivese, M.; Orlando, P.; Di Marzo, V. *Exp. Cell Res.* **2007**, *313*, 1911−1920.

(21) Macpherson, L. J.; Hwang, S. W.; Miyamoto, T.; Dubin, A. E.; Patapoutian, A.; Story, G. M. *Mol. Cell Neurosci.* **2006**, *32*, 335−343.

(22) Voets, T.; Owsianik, G.; Janssens, A.; Talavera, K.; Nilius, B. *Nat. Chem. Biol.* **2007**, *3*, 174−182.

(23) Brauchi, S.; Orta, G.; Salazar, M.; Rosenmann, E.; Latorre, R. *J. Neurosci.* **2006**, *26*, 4835−4840.

(24) Malkia, A.; Pertusa, M.; Fernandez-Ballester, G.; Ferrer-Montiel, A.; Viana, F. *Mol. Pain* **2009**, *5*, 62.

(25) Ramachandran, R.; Hyun, E.; Zhao, L.; Lapointe, T. K.; Chapman, K.; Hirota, C. L.; Ghosh, S.; McKemy, D. D.; Vergnolle, N.; Beck, P. L.; Altier, C.; Hollenberg, M. D. *Proc. Natl. Acad. Sci. U.S.A.* **2013**, *110*, 7476−7481.

(26) Holzer, P. *Pharmacol. Ther.* **2011**, *131*, 142−170.

(27) Kimball, E. S.; Wallace, N. H.; Schneider, C. R.; D'Andrea, M. R.; Hornby, P. J. *Neurogastroenterol. Motil.* **2004**, *16*, 811−818.

(28) Nozawa, K.; Kawabata-Shoda, E.; Doihara, H.; Kojima, R.; Okada, H.; Mochizuki, S.; Sano, Y.; Inamura, K.; Matsushime, H.; Koizumi, T.; Yokoyama, T.; Ito, H. *Proc. Natl. Acad. Sci. U.S.A.* **2009**, *106*, 3408−3413.

(29) DeFalco, J.; Duncton, M. A.; Emerling, D. *Curr. Top. Med. Chem.* **2011**, *11*, 2237−2252.

(30) Gunthorpe, M. J.; Szallasi, A. *Curr. Pharm. Des.* **2008**, *14*, 32−41.

(31) Romanovsky, A. A.; Almeida, M. C.; Garami, A.; Steiner, A. A.; Norman, M. H.; Morrison, S. F.; Nakamura, K.; Burmeister, J. J.; Nucci, T. B. *Pharmacol. Rev.* **2009**, *61*, 228−261.

(32) Garami, A.; Shimansky, Y. P.; Pakai, E.; Oliveira, D. L.; Gavva, N. R.; Romanovsky, A. A. *J. Neurosci.* **2010**, *30*, 1435−1440.

(33) Kort, M. E.; Kym, P. R. *Prog. Med. Chem.* **2012**, *51*, 57−70.

(34) Almeida, M. C.; Hew-Butler, T.; Soriano, R. N.; Rao, S.; Wang, W.; Wang, J.; Tamayo, N.; Oliveira, D. L.; Nucci, T. B.; Aryal, P.; Garami, A.; Bautista, D.; Gavva, N. R.; Romanovsky, A. A. *J. Neurosci.* **2012**, *32*, 2086−2099.

(35) Jenkinson, D. H. In *Textbook of Receptor Pharmacology*; Foreman, J. C.; Johansen, T.; Gibb, A. J., Eds.; CRC Press: Boca Raton, FL, 2011; Chapter 1, pp 41−46.

(36) Valenzano, K. J.; Grant, E. R.; Wu, G.; Hachicha, M.; Schmid, L.; Tafesse, L.; Sun, Q.; Rotshteyn, Y.; Francis, J.; Limberis, J.; Malik, S.; Whittemore, E. R.; Hodges, D. *J. Pharmacol. Exp. Ther.* **2003**, *306*, 377−386.

(37) Gunthorpe, M. J.; Rami, H. K.; Jerman, J. C.; Smart, D.; Gill, C. H.; Soffin, E. M.; Luis Hannan, S.; Lappin, S. C.; Egerton, J.; Smith, G. D.; Worby, A.; Howett, L.; Owen, D.; Nasir, S.; Davies, C. H.; Thompson, M.; Wyman, P. A.; Randall, A. D.; Davis, J. B. *Neuropharmacology* **2004**, *46*, 133−149.

(38) Cui, M.; Honore, P.; Zhong, C.; Gauvin, D.; Mikusa, J.; Hernandez, G.; Chandran, P.; Gomtsyan, A.; Brown, B.; Bayburt, E. K.; Marsh, K.; Bianchi, B.; McDonald, H.; Niforatos, W.; Neelands, T.

R.; Moreland, R. B.; Decker, M. W.; Lee, C. H.; Sullivan, J. P.; Faltynek, C. R. *J. Neurosci.* **2006**, *26*, 9385−9393.